

# Realization of Scaled Admittance Bilateral Control with Different Inertias Using Piezoelectric Actuator

1<sup>st</sup> Saki Kozu

Graduate School of  
Integrated Design Engineering  
Keio University  
Yokohama, Japan  
kozu@sum.sd.keio.ac.jp

2<sup>nd</sup> Izumi Kotani

Graduate School of  
Integrated Design Engineering  
Keio University  
Yokohama, Japan  
kotani@sum.sd.keio.ac.jp

3<sup>rd</sup> Kenta Seki

Department of Electrical and Mechanical Engineering  
Nagoya Institute of Technology  
Nagoya, Japan  
k-seki@nitech.ac.jp

4<sup>th</sup> Naoki Motoi

Graduate School of Maritime Science  
Kobe University  
Kobe, Japan  
motoi@maritime.kobe-u.ac.jp

5<sup>th</sup> Takahiro Nozaki

Department of System Design Engineering  
Keio University  
Yokohama, Japan  
nozaki@sd.keio.ac.jp

**Abstract**—In micro-manipulations such as cell manipulation, it is desirable for the operator to feel the haptic sensation of the object. Bilateral control can remotely transmit position and force information between leader and follower systems. In this control, the use of a linear motor as a leader and a stacked piezoelectric actuator as a follower has been proposed to achieve micro-scale operation. There is a lot that needs to be clarified about bilateral control when the structure differs between leader and follower systems. In conventional scaled 4-channel (4ch) bilateral control, a theory of oblique coordinate control has been proposed that considers differences in the inertia of leader and follower systems. However, when a piezoelectric actuator is used, the control scheme differs from using two linear motors with different inertias because the structures of the leader and follower systems are entirely different. Another method is scaled admittance bilateral control. However, the control design when structures and inertias of the two systems are different has not yet been clarified. In this paper, a scaled admittance bilateral control using a piezoelectric actuator and a linear motor is constructed. Experiments confirm that the realized scaled admittance bilateral control has the equivalent position and force tracking performances as the conventional scaled 4ch bilateral control using a piezoelectric actuator. Furthermore, the designed scaled admittance bilateral control is more robust to fluctuations in the nominal inertia of the piezoelectric actuator than the conventional scaled 4ch bilateral control.

**Index Terms**—Scaled bilateral control, micro-manipulation, piezoelectric actuator

## I. INTRODUCTION

Cell manipulations, such as transplantation and removal of nuclei, are required in vitro fertilization and Coulomb technology. Currently, those operations are performed manually by skilled operators, and it is inefficient and difficult to treat tiny cells on the micro-scale.

Microfluidic devices [1], optical tweezers [2], magnetic tweezers [3], and acoustic tweezers [4] have been studied for micro-manipulation. Such non-contact manipulations can only

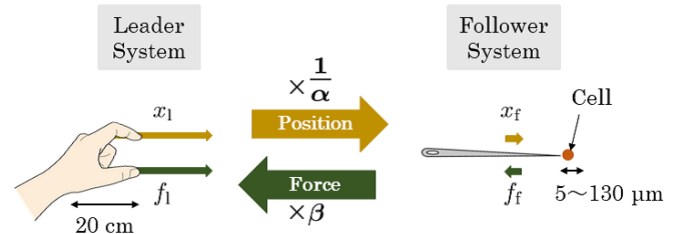


Fig. 1: Scaled bilateral control.

trap cells' positions, and manipulations in the nucleus and cytoplasm are difficult. Precision manipulators have also been proposed for cell manipulations. [5], [6]. However, these have high impedance due to position-controlled manipulation and may destroy soft cells.

To solve these problems, scaled bilateral control has been proposed, in which the position and the force information is remotely transmitted between a human-operated leader system and a micro-manipulated follower system by scaling up or down [7]. The operator can feel the environmental contact force of the follower system. In scaled bilateral control, the use of a linear motor as a leader for human manipulation and a stacked piezoelectric actuator as a follower for precise manipulation has been proposed [8], [9]. A stacked piezoelectric actuator has advantages in micro-scale operations because it is frictionless and fast-responding. On the other hand, they have nonlinearities such as hysteresis and creep phenomena. These had made modeling piezoelectric actuators difficult. However, a disturbance observer (DOB) design has made it possible to construct a control system that can compensate for the nonlinearities [10].

In previous studies, scaled 4-channel (4ch) bilateral control was constructed using a piezoelectric actuator [8], [9]. In

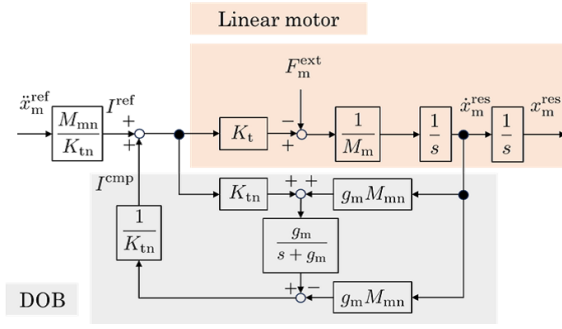


Fig. 2: Acceleration control of linear motor.

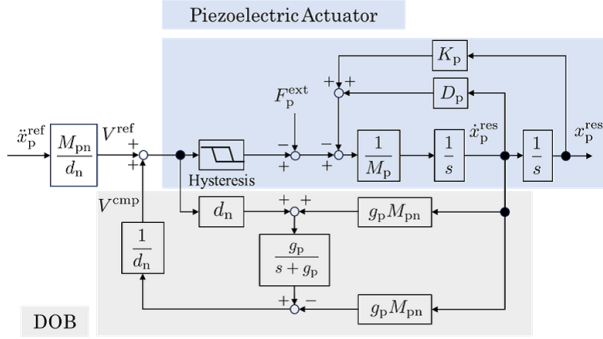


Fig. 3: Acceleration control of piezoelectric actuator.

4ch bilateral control, a theory of oblique coordinate control has been proposed that considers differences in the inertia of the leader and follower systems [11]. However, it is difficult to accurately identify the inertia of a piezoelectric actuator. Because stiffness is extremely large and the inertial behavior of a piezoelectric actuator is different from the inertia obtained by a weighing machine [12]. Piezoelectric actuators are not actuated by overall movement but by distortion when voltage is applied. Furthermore, when a piezoelectric actuator and a linear motor are used, the control scheme differs from oblique coordinate control using two linear motors because the structures of leader and follower systems are entirely different.

As another design of bilateral control, admittance bilateral control has been proposed [13]. However, the design of the scaled admittance bilateral control scheme, especially when the structures and inertias of the two systems are different, has not been examined. This paper constructs a scaled admittance bilateral control using a linear motor and a piezoelectric actuator. The control scheme can be designed without considering the difference in structure and inertia of the two systems in position and force transmissions.

The performances and robustness of the conventional scaled 4ch bilateral control and the designed scaled admittance bilateral control are compared through experiments.

The remainder of this paper is as follows. Section II describes the control design of the scaled 4ch bilateral control and the scaled admittance bilateral control using a piezo-

TABLE I: Parameters of linear motor.

$I^{ref}$	Current reference
$I^{cmp}$	Current compensation
$g_m$	Cutoff frequency of observer
$K_t$	Torque constant
$K_{tn}$	Nominal torque constant
$M_m$	Inertia
$M_{mn}$	Nominal inertia
$x_m^{res}$	Position response
$F_m^{ext}$	Reaction force

TABLE II: Parameters of piezoelectric actuator.

$V^{ref}$	Voltage reference
$V^{cmp}$	Voltage compensation
$g_p$	Cutoff frequency of observer
$d_n$	Nominal constant between voltage and generated force
$M_p$	Inertia
$M_{pn}$	Nominal inertia
$K_p$	Stiffness
$D_p$	Viscosity
$x_p^{res}$	Position response
$F_p^{ext}$	Environmental contact force

electric actuator and a linear motor. Section III shows the experimental results, and section IV concludes this paper.

## II. CONTROL SYSTEM

### A. Scaled bilateral control

Fig. 1 shows the schematic diagram of the scaled bilateral control. When the operator moves the leader position  $x_l$ , the displacement  $x_f$  is generated on the follower. Furthermore, when the follower contacts the environment and a reaction force  $f_f$  is generated, the force  $f_l$  is transmitted to the operator.  $\alpha$  and  $\beta$  are the position and force scaling factors, and the operator can correctly sense the environmental impedance when these values are set equal. The control target of scaled bilateral control is

$$x_l - \alpha x_f = 0, \quad (1)$$

$$f_l + \beta f_f = 0. \quad (2)$$

For example, the size of a human cell is 5 to 130  $\mu\text{m}$ . The human hand is approximately 20 cm, and this paper considers scaling factors of 100 to 1000 appropriate for the desired cell manipulation.

### B. Motion control of linear motor and piezoelectric actuator

In bilateral control, acceleration references are given to each system. The acceleration control shown in Fig. 2 and Fig. 3 are constructed for a linear motor and a piezoelectric actuator. The definitions of parameters are shown in Table I and Table II.

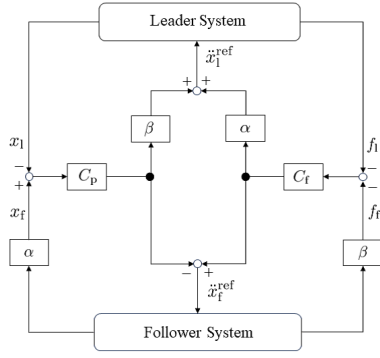


Fig. 4: Scaled 4ch bilateral control.

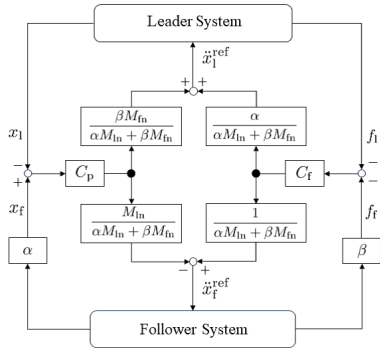


Fig. 5: Scaled 4ch bilateral control considering difference in inertia.

It is difficult to build bilateral control because the structures of the two systems are different. For example, a linear motor is current-driven, while a piezoelectric actuator is voltage-driven. Furthermore, inertia is dominant in a linear motor, while stiffness is dominant in a piezoelectric actuator.

DOB is designed for both systems to suppress the disturbance force, such as viscosity and stiffness. The reaction force observer (RFOB) is designed for the linear motor to estimate the operator's reaction force  $\hat{F}_m^{ext}$  [10].

### C. Scaled 4ch bilateral control

Scaled 4ch bilateral control is one of the control schemes able to satisfy (1) and (2).

When the inertias of the two systems are equal, the block diagram is shown in Fig. 4, where  $C_p$  and  $C_f$  are the position controller and the force controller,  $\ddot{x}_l^{ref}$  and  $\ddot{x}_f^{ref}$  are the acceleration references given to leader and follower systems, respectively [7].

When the inertias of the two systems are different, the block diagram is shown in Fig. 5, considering the difference between inertia  $M_{ln}$  on the leader and inertia  $M_{fn}$  on the follower [11].

However, the block diagram of the conventional scaled 4ch bilateral control using a piezoelectric actuator and a linear motor is shown in Fig. 6, different from Fig. 5 [9]. Where  $C_{pm}$  and  $C_{pp}$  are position controllers and  $C_{fm}$  and  $C_{fp}$  are force controllers respectively. It is necessary to separately design two

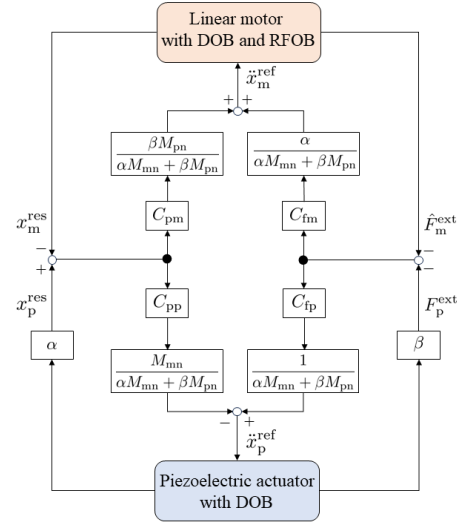


Fig. 6: Scaled 4ch bilateral control using linear motor and piezoelectric actuator.

position and force controllers with different orders because the structures of the two systems are completely different. Furthermore, the controllers are designed for the difference in position and the sum of forces between the two systems with vastly different bandwidths.

The acceleration reference given to the linear motor  $s^2 x_m^{ref}$  and piezoelectric actuator  $s^2 x_p^{ref}$  are

$$\begin{bmatrix} s^2 x_m^{ref} \\ s^2 x_p^{ref} \end{bmatrix} = \begin{bmatrix} \frac{1}{\alpha M_{mn} + \beta M_{pn}} \{ \beta M_{pn} C_{pm} (\alpha x_p^{res} - x_m^{res}) - \alpha C_{fm} (\hat{F}_m^{ext} + \beta F_p^{ext}) \} \\ \frac{1}{\alpha M_{mn} + \beta M_{pn}} \{ M_{mn} C_{pp} (x_m^{res} - \alpha x_p^{res}) - C_{fp} (\hat{F}_m^{ext} + \beta F_p^{ext}) \} \end{bmatrix} \quad (3)$$

### D. Scaled admittance bilateral control

Scaled admittance bilateral control is also a control schemes that satisfies (1) and (2). The force controller is designed for the sum of forces, the same as the scaled 4ch bilateral control. On the other hand, the position controllers are separately designed for the leader and the follower systems.

The scaled admittance bilateral control constructed in this paper is shown in Fig. 7. The structure in Fig. 7 is equivalent to the scaled admittance bilateral control in which the inertias of the two systems are equal.

The virtual admittance  $Y$  is as

$$Y = \frac{1}{M_d s + D_d}, \quad (4)$$

where  $M_d$  and  $D_d$  are the virtual inertia and the virtual viscosity,  $s$  is the Laplace operator, respectively. Here,  $M_d$  in the admittance bilateral control is equivalent to the inverse of the force controller  $C_f$  in the 4ch bilateral control. Admittance controllers are prone to hunting because they have position controllers in the internal loop. Thus, a viscosity term  $D_d$  is added to suppress it.

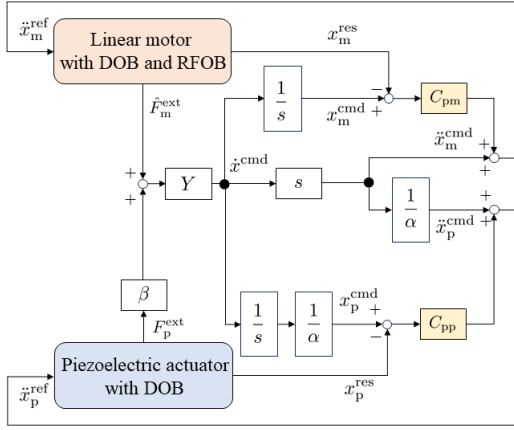


Fig. 7: Scaled admittance bilateral control using linear motor and piezoelectric actuator.

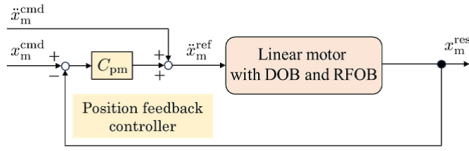


Fig. 8: Position controller of linear motor.

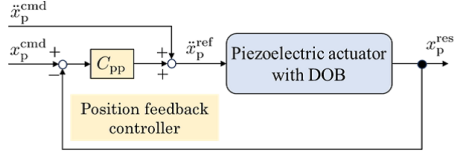


Fig. 9: Position controller of piezoelectric actuator.

The velocity command  $sx^{\text{cmd}}$  is generated as

$$sx^{\text{cmd}} = Y(\hat{F}_m^{\text{ext}} + \beta F_p^{\text{ext}}). \quad (5)$$

The velocity command becomes a virtual admittance motion with the sum of the reaction force of the linear motor  $\hat{F}_m^{\text{ext}}$  and the environmental force of the piezoelectric actuator  $F_p^{\text{ext}}$ . The position commands given to the linear motor and the piezoelectric actuator are  $x_m^{\text{cmd}}$  and  $x_p^{\text{cmd}}$ , considering the position scaling factor  $\alpha$ .

Position and velocity feedback control and acceleration feed-forward control are separately constructed for each system's command. Thus, individually designed position controllers for a linear motor  $C_{pm}$  and a piezoelectric actuator  $C_{pp}$  shown in Fig. 8 and Fig. 9 can be used as controllers for the admittance bilateral control. It is evident because Fig. 7 contains the same structures as Fig. 8 and Fig. 9.

From the above, the acceleration references given to the linear motor  $s^2x_m^{\text{ref}}$  and the piezoelectric actuator  $s^2x_p^{\text{ref}}$  are

$$\begin{bmatrix} s^2x_m^{\text{ref}} \\ s^2x_p^{\text{ref}} \end{bmatrix} = \begin{bmatrix} C_{pm}(x_m^{\text{cmd}} - x_m^{\text{res}}) + s^2x_m^{\text{cmd}} \\ C_{pp}(\frac{1}{\alpha}x_p^{\text{cmd}} - x_p^{\text{res}}) + \frac{1}{\alpha}s^2x_p^{\text{cmd}} \end{bmatrix}. \quad (6)$$

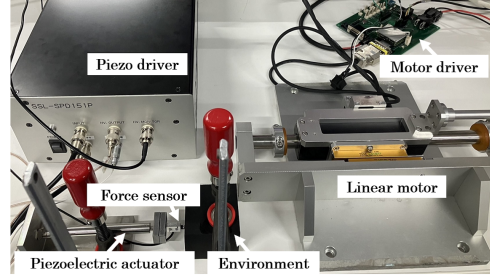


Fig. 10: Experimental devices.

TABLE III: Linear motor and piezoelectric actuator parameters.

$M_{mn}$	0.55 kg
$M_{pn}$	0.01 kg
$K_{tn}$	6.0 Nm/A
$d_n$	4.9 N/V
$g_m$	500 rad/s
$g_p$	500 rad/s

### III. EXPERIMENTS

#### A. Experimental conditions

The experimental devices are shown in Fig. 10. A rubber block was fixed to the desk as an environment on the piezoelectric actuator side. A strain gauge and a load cell measured the position and force of the piezoelectric actuator.

In the experiment, the linear motor was operated from a free state just before the piezoelectric actuator made contact with the rubber block. Contact between the piezoelectric actuator and the environment was repeated by position tracking.

The linear motor and piezoelectric actuator parameters are shown in Table III. For the piezoelectric actuator, the previous study using the same actuator was referenced [8].

The controllers shown in Fig. 6 and Fig. 7 were designed when both scaling factors  $\alpha$  and  $\beta$  were 100, as shown in Table IV and Table V. The position controllers include PD gains, and the force controllers include P gains. Each gain was set as high as possible without destabilizing, and the virtual inertia and virtual viscosity were set as low as possible.

#### B. Performances of two controllers

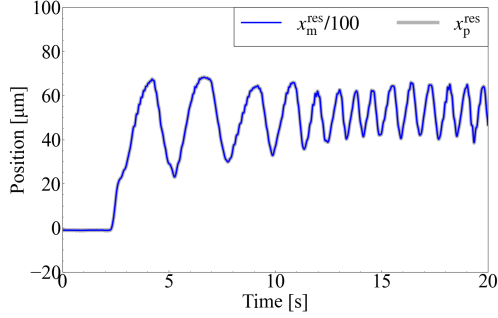
The position and force responses of the scaled 4ch bilateral control and scaled admittance bilateral control, when both scaling factors  $\alpha$  and  $\beta$  were 100, are shown in Fig. 11 and Fig. 12. The piezoelectric actuator's displacement and force were almost 1/100 of the linear motor. Thus, the constructed scaled admittance bilateral control using a piezoelectric actuator achieved equivalent position and force-tracking performance as the conventional scaled 4ch bilateral control.

#### C. Robustness of two controllers

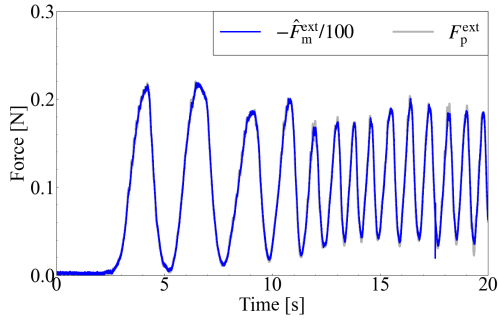
1) *Scaling factors change*: Experiments were conducted with scaling factors  $\alpha$  and  $\beta$  were 1000, and position and force tracking were confirmed for both 4ch bilateral control and admittance bilateral control. The admittance bilateral control

**TABLE IV:** Design of scaled 4ch bilateral control.

$K_{pm}$	Position gain of $C_{pm}$	$1.2 \times 10^4$ 1/s <sup>2</sup>
$K_{dm}$	Velocity gain of $C_{pm}$	$5.0 \times 10^3$ 1/s
$K_{pp}$	Position gain of $C_{pp}$	$8.0 \times 10^8$ 1/s <sup>2</sup>
$K_{dp}$	Velocity gain of $C_{pp}$	$2.0 \times 10^6$ 1/s
$K_{fm}$	Force gain of $C_{fm}$	0.2 m/Ns <sup>2</sup>
$K_{fp}$	Force gain of $C_{fp}$	20 m/Ns <sup>2</sup>



(a) Position response.



(b) Force response.

**Fig. 11:** Experimental result of scaled 4ch bilateral control ( $\alpha, \beta = 100$ ,  $M_{pn} = 0.01$ ).

constructed in this experiment had the same structure as the one without considering the difference in the inertia of the two systems. However, the control structure was found to be valid experimentally.

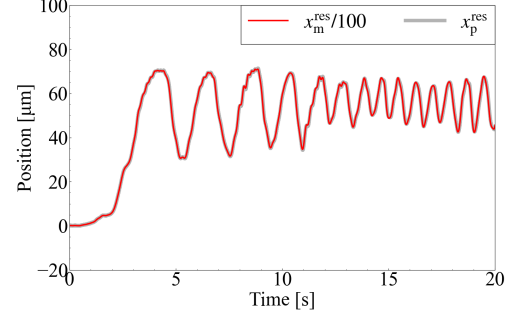
2) *Nominal inertia of piezoelectric actuator change:* Further experiments were conducted with the nominal inertia of the piezoelectric actuator  $M_{pn}$  set to twice the value shown in Table III.

In the scaled 4ch bilateral control, as shown in Fig. 13, the amplitude of high frequency vibration of the force increased as nominal inertia was increased. Furthermore, the system became unstable when  $M_{pn}$  was more than seven times the value shown in Table III. This may be because the change in nominal inertia of the piezoelectric actuator affected the force control in the control system shown in Fig. 6.

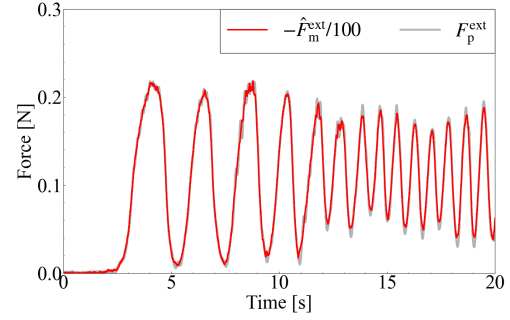
In the scaled admittance control, as shown in Fig. 14, there was no significant difference from the shape of position

**TABLE V:** Design of scaled admittance bilateral control.

$K_{pm}$	Position gain of $C_{pm}$	1600 1/s <sup>2</sup>
$K_{dm}$	Velocity gain of $C_{pm}$	100 1/s
$K_{pp}$	Position gain of $C_{pp}$	$5.0 \times 10^8$ 1/s <sup>2</sup>
$K_{dp}$	Velocity gain of $C_{pp}$	$1.25 \times 10^6$ 1/s
$M_d$	Virtual inertia	10 kg
$D_d$	Virtual viscosity	20 Ns/m



(a) Position response.



(b) Force response.

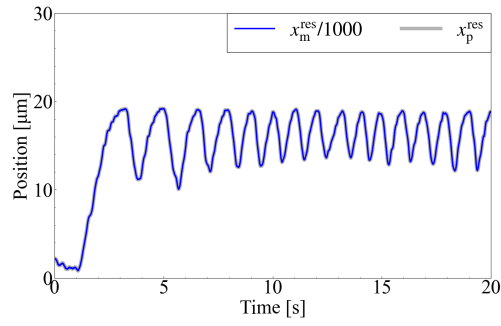
**Fig. 12:** Experimental result of scaled admittance bilateral control ( $\alpha, \beta = 100$ ,  $M_{pn} = 0.01$ ).

and force responses shown in Fig. 12. The part of the force response that is not sharp may be due to the effect of the virtual viscosity and the increase in nominal inertia. Even when  $M_{pn}$  was increased ten times, the control system still operated, although the feeling of operation became heavier. Therefore, the designed admittance bilateral control is robust to fluctuations in the nominal inertia of the piezoelectric actuator.

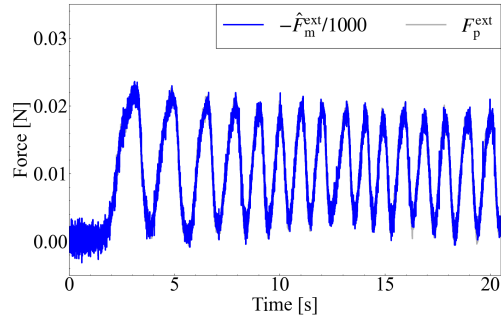
#### IV. CONCLUSIONS

The scaled admittance bilateral control design when the systems and inertias of the two systems were different had not been clarified. In this research, the same scaled admittance bilateral control system as when the inertias of the two systems are equal was able to be used with a piezoelectric actuator and a linear motor. Experiments confirmed that the constructed scaled admittance bilateral control had the equivalent position



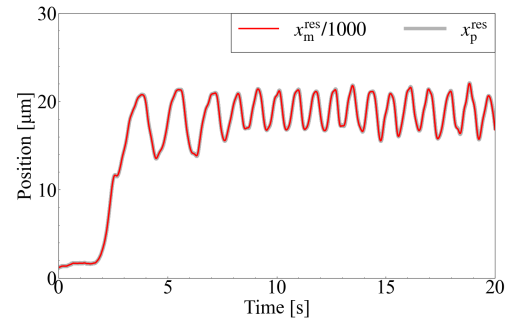


(a) Position response.

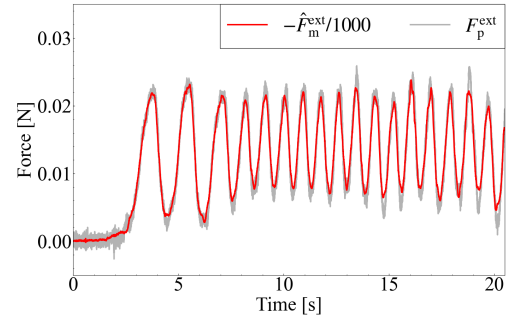


(b) Force response.

**Fig. 13:** Experimental result of scaled 4ch bilateral control ( $\alpha, \beta = 1000$ ,  $M_{pn} = 0.02$ ).



(a) Position response.



(b) Force response.

**Fig. 14:** Experimental result of scaled admittance bilateral control ( $\alpha, \beta = 1000$ ,  $M_{pn} = 0.02$ ).

and force tracking performances as the conventional scaled 4ch bilateral control. Furthermore, The designed scaled admittance bilateral control was more robust to fluctuations in the nominal inertia of the piezoelectric actuator than the conventional scaled 4ch bilateral control. The results will contribute to studying scaled bilateral control using two different systems, especially a piezoelectric actuator.

## REFERENCES

- [1] Y. Liu, D. Ren, X. Ling, W. Liang, J. Li, X. You, Y. Yalikun, and Y. Tanaka, "Time sequential single-cell patterning with high efficiency and high density", *Sensors*, vol. 18, no. 11, Oct. 2018.
- [2] Z. Zhang, T. E. P. Kimkes, and M. Heinemann, "Manipulating rod-shaped bacteria with optical tweezers", *Scientific Reports*, vol. 9, Dec. 2019.
- [3] M. Hagiwara, T. Kawahara, Y. Yamanishi, T. Masuda, L. Feng, and F. Arai, "On-chip magnetically actuated robot with ultrasonic vibration for single cell manipulations", *Lab on a Chip*, vol. 11, no. 12, pp. 2049–2054, June 2011.
- [4] L. Huang, D. Tang, J. Qian, and H. Xia, "An octagonal acoustofluidic device for multimode cell and particle patterning and dynamical manipulation", *IEEE Sensors Journal*, vol. 23, no. 7, pp. 6589–6595, Apr. 2023.
- [5] C. Dai, Z. Zhang, Y. Lu, G. Shan, X. Wang, Q. Zhao, C. Ru, and Yu Sun, "Robotic manipulation of deformable cells for orientation control", *IEEE Transaction on Robotics*, vol. 36, no. 1, pp. 271–283, Feb. 2020.
- [6] M. Xie, A. Shakoor, Y. Shen, J. K. Mills, and D. Sun, "Out-of-plane rotation control of biological cells with a robot-tweezers manipulation system for orientation-based cell surgery," *IEEE Transactions on Biomedical Engineering*, vol. 66, no. 1, pp. 199–207, Jan. 2019.
- [7] W. Iida and K. Ohnishi, "Reproducibility and operationality in bilateral teleoperation", in *Proc. of The 8th IEEE International Workshop on Advanced Motion Control*, pp. 217–222, 2004.
- [8] S. Yamaoka, T. Nozaki, D. Yashiro, and K. Ohnishi, "Acceleration control of stacked piezoelectric actuator utilizing disturbance observer and reaction force observer", in *Proc. of The 12th IEEE International Workshop on Advanced Motion Control*, pp. 1–6, Mar. 2012.
- [9] K. Murakumo and N. Motoi, "Stiffness measurement method based on micro-macro bilateral control for micro-order objects", in *Proc. of Mechatronics and AISM*, Sep. 2023.
- [10] E. Sariyildiz and K. Ohnishi, "Stability and Robustness of Disturbance-Observer-Based Motion Control Systems", *IEEE Transactions on Industrial Electronics*, vol. 62, no. 1, pp. 414–422, Jan. 2015.
- [11] S. Sakaino, T. Sato, and K. Ohnishi, "Multi-DOF micro-macro bilateral controller using oblique coordinate control", *IEEE Transactions on Industrial Informatics*, vol. 7, no. 3, pp. 446–454, Aug. 2011.
- [12] H. Adriaens, W. L. De Koning, and R. Banning, "Modeling piezoelectric actuators", *IEEE Transactions on Mechatronics*, vol. 5, no. 4, pp. 331–341, Dec. 2000.
- [13] Y. Nagatsu and H. Hashimoto, "Bilateral control by transmitting force information with application to time-delay systems and human motion reproduction", *IEEE Journal of Industry Applications* vol. 10, no. 2, pp. 165–177, Jan. 2021.